EXPERIMENTAL EVALUATION OF MULTI-PHY 6TISCH NETWORKS

Milica Lekić[1], Gordana Gardašević[1], Milan Mlađen[1]
[1]University of Banja Luka, Faculty of Electrical Engineering, Patre 5, 78 000 Banja Luka, Bosnia and Herzegovina

NOTE: Corresponding author: Gordana Gardašević, gordana.gardasevic@etf.unibl.org

Abstract – *The architectural design of Wireless Sensor Networks (WSNs) for the Industrial Internet of Things (IIoT) applications requires the careful planning and selection of an appropriate operational strategy. Harmonization of standards is crucial to ensure easier certification and commercialization of IIoT solutions. The ongoing research activities are directed toward designing agile, reliable, and secure transmission technologies and protocols. Recently, Time Slotted Channel Hopping (TSCH) standardization bodies have started to consider support for multiple physical layers thus accommodating a wide range of applications. This paper presents the results of the extensive experimental measurement campaign to study the performance of the 6TiSCH (IPv6 over the TSCH mode of IEEE 802.15.4e) network while supporting multiple physical layers (PHYs). For measurement purposes, all experiments were performed on OpenMote-B hardware. These devices are equipped with an Atmel AT86RF215 dual radio transceiver implementing IEEE 802.15.4g. The performance evaluation is provided for the following metrics: network formation time, Packet Delivery Ratio (PDR), latency, and duty cycle. Results are encouraging, particularly in terms of high PDR for all tested PHYs. Performance evaluation indicates the importance of proper node positioning, link quality estimation and careful selection of network parameters. Moreover, collected experimental results create a dataset that provides insights into the tested PHYs' performance and their potential for indoor 6TiSCH networking.*

Keywords – 6TiSCH, IEEE 802.15.4g, industrial IoT, multiple PHYs, OpenMote-B

1. INTRODUCTION

The adoption of the Industrial Internet of Things (IIoT) standards and protocols plays a key role in accelerating the transformation of traditional systems into a new generation known as Industry 4.0 [1]. Cyber-Physical Systems (CPSs) will enable the advanced monitoring of physical processes, as well as the creation of virtual resources and decentralized decision-making. In the context of Industry 4.0, a special challenge is to achieve adequate transmission performance in terms of response time, delays, reliability, and process automation, possibly without human intervention. Wireless Sensor Networks (WSNs) provide the infrastructure for a large number of IIoT applications, starting from automation and control of industrial processes, to large smart grid systems in power plants and intelligent transportation systems. In order to support the more dynamic and heterogeneous scenarios, the new generation of IIoT applications will be driven by advanced technologies, such as Artificial Intelligence (AI) and Machine Learning (ML) [2, 3], big data analytics [4, 5], Fog/Edge computing [6, 7], cybersecurity [8, 9], blockchain [10, 11], Software Defined Networking (SDN) [12, 13], etc. It is expected that their use will significantly reduce operating costs and increase overall work efficiency.

Standardization of IIoT architectures and the corresponding protocol-stack design are of particular importance. Research in this area has enabled advanced solutions and mechanisms, especially in the physical (PHY) and Medium Access Control (MAC) layers, as well as optimization of routing protocols, energy-efficient data processing and transmission techniques, and integration of novel technologies into industrial WSN networks. Transmission characteristics in the field of industrial automation are such that it is necessary to provide guaranteed performance and reliability.

Time-Slotted Channel Hopping (TSCH) [14] has been introduced as a synchronous medium access control protocol in the IEEE 802.15.4e [15] standard. It has attracted considerable attention from the research community as it promises low-power, deterministic, reliable and predictable operations, particularly for the challenging IIoT environments. The IPv6 over the TSCH mode of IEEE 802.15.4e (6TiSCH) architecture [16] provides some unique properties, such as high energy efficiency and extremely high transmission reliability, efficient WSN mesh networking, and a fully standardized protocol stack. This technology is recognized as one of the candidates for the reference WSN radio technology in future IIoT networks. Moreover, 6TiSCH is based on open standards, with support for different scheduling strategies, as well as for deterministic packet switching over the TSCH MAC sublayer. The continuation of standardization activities has resulted in the standard revision IEEE 802.15.4-2015 [17] which includes the variety of PHYs, each targeting specific applications and market segments [18, 19].

Development of IoT technologies for long-distance transmission has enabled the implementation of specific applications, such as Advanced Metering Infrastructure (AMI), smart utilities, etc. An important requirement also relates to the need to ensure long battery life, as well as two-way communication that can be controlled remotely. In order

to meet these requirements, specifications for Wireless Smart Utility Networks (Wi-SUNs) have been introduced. Wi-SUNs have two significant features: low power transmission and support for bidirectional multihop transmission. These systems are based on the IEEE 802.15.4g standard [20] which describes a new set of PHYs based on three modulation techniques operating in sub-GHz and 2.4 GHz bands [21, 22] thus introducing the modulation diversity. The objective of our paper is to provide an experimental comparison of IEEE802.15.4g physical layers in 6TiSCH networks. For wide adoption of 6TiSCH technology, a seamless integration of industrial WSNs and Internet must be provided.

The current limitations in terms of network formation strategies, as well as joining procedures and synchronization need to be addressed and overcome. The diversity of PHYs in IEEE 802.15.4g makes this challenge even more complex. Based on this, our motivation is to examine and evaluate performances of multi-PHY 6TiSCH networks under different configurations. The main contributions of this paper are the following:

- Firstly, we provide an overview of the recent related work based on experimental platforms;
- Secondly, we present a detailed description of the experimental setup based on open hardware and open software platforms;
- Lastly, a thorough performance evaluation and discussion has been given.

The rest of the paper is organized as follows. Section 2 provides the overview of related work. Section 3 introduces recent trends and technologies recognized as key enablers for future deterministic IIoT networking. Synchronous MAC scheduling in IEEE 802.15.4e - TSCH, and IEEE 802.15.4g are discussed in particular. Details on experimental campaign and methodology are described in Section 4. The experimental results are presented in Section 5. Section 6 reflects key findings and observations related to obtained results. Finally, the conclusion highlights key observations and future work.

2. RELATED WORK

This section presents a survey of the work related to IEEE 802.15.4g and modulation diversity applied in 6TiSCH networks.

Authors in [23] introduce g6TiSCH as a generalization of the standardized IETF 6TiSCH protocol stack. The experimentation has been performed by using nodes equipped with multiple radios having the ability to dynamically switch between them on a link-by-link basis. For the performance evaluation, OpenMote-B boards were deployed in an indoor office, where network formation time, end-to-end reliability, end-to-end latency, and battery lifetime were measured. The comparison of g6TiSCH and a traditional 6TiSCH stack has been provided.

In [24], the characterization of 6TiSCH performance when using different PHYs has been provided. The initial OpenWSN implementation has been extended to support one of three physical layers from the IEEE802.15.4g standard: FSK 868 MHz, OFDM 868 MHz, and O-QPSK 2.4 GHz. Results encourage the use of the generalized 6TiSCH architecture in which technology-agile radio chips are driven by a protocol stack which chooses the most appropriate PHY on a frame-by-frame basis.

In [25], the experimental performance evaluation of the IEEE 802.15.4g applications has been conducted in three test scenarios using the OpenMote-B hardware and RIOT software platforms. The overall results present a dataset obtained from the deployment of two nodes using the IEEE 802.15.4g SUN modulations. The following metrics were used for data traffic analysis: packet loss [%], average Received Signal Strength Indicator (RSSI) [dBm], min/avg/max Round Trip Time (RTT) [ms], and PHY configuration.

Authors in [26] have analyzed the suitability of the IEEE 802.15.4g technology for real-life IoT applications in different contexts. A set of experimental measurements has been performed both in rural and urban environments, to evaluate the communication range and the packet delivery ratio. For experimental purposes, the testbed deployed Zolertia sensor nodes equipped with a CC1120 radio transceiver operating at an 868 MHz band with 2-Gaussian Frequency Shift Keying (GFSK) modulation and 33 channels available, with a bit rate of 50 kbps, and running the Contiki operating system. Results obtained show that, in a real environment, communication may be strongly affected by the presence of buildings, trees, and other obstacles in the area. Results have shown that in an urban scenario the communication range is below 200 m, while in a rural environment it is possible to cover distances in the order of 800 m.

Two alternative timeslot structures allowing multiple packet transmissions to increase the throughput for higher data rate PHYs have been proposed in [27]. The paper provides theoretical evaluation of the proposed slot structures in terms of throughput, energy consumption and memory constraints, as well as an experimental validation in a real-world testbed with 33 Zolertia RE-Motes spanning three floors and covering an area of 2550 m^2. Results confirm that by using adaptive multi-PHY TSCH, a stable network can be established maximizing throughput and minimizing the number of hops by using both high throughput and reliable links.

The adaptive modulation diversity selection strategy which allows to dynamically select different modulations in order to improve link reliability has been proposed in [21]. Based on the simulation results obtained with a real-world dataset using the IEEE 802.15.4g SUN modulations (i.e. SUN-FSK, SUN OQPSK and SUN-OFDM) in an industrial environment, applying any modulation diversity strategy allows an increase in the Packet Delivery Ratio (PDR) with respect to using a single modulation.

Table 1 provides a brief summary of the related work presented in this section.

Table 1 – Summary of related work

APPLICATION	ENVIRONMENT	PLATFORMS	PERFORMANCE METRICS	REF.
Dynamic PHY selection	indoor office	OpenMote-B and OpenWSN	network formation time, end-to-end reliability, end-to-end latency, battery lifetime	[23]
PHY change on frame-by-frame basis	indoor office	OpenMote-B and OpenWSN	network formation time, end-to-end reliability, end-to-end latency, radio duty cycle	[24]
All PHY configurations tested	indoor	OpenMote-B and RIOT	packet loss, average RSSI, min/avg/max RTT	[25]
Testing the suitability of the IEEE 802.15.4g for real-life IoT applications in different scenarios	urban, rural outdoor	Zolertia and Contiki	range, PDR	[26]
Adaptive multi-PHY TSCH approach based on two proposed timeslot structures tested for higher-data-rate PHYs	indoor	Zolertia and Contiki-NG (imec Wireless Officelab)	throughput, energy consumption, memory constraints	[27]
Adaptive PHY modulation selection against link reliability	industrial indoor	OpenMote-B and Python simulator	PDR and RNP	[21]

3. TOWARDS RELIABLE AND DETERMINISTIC IIOT NETWORKING

Accelerated development of IIoT standards has enabled the connection of traditional industrial systems with Internet networks. In particular, for the IEEE 802.15.4e standard, special attention is paid to IPv6 communication in TSCH-based networks, in order to integrate industrial sensor devices into IP environments. However, such integration introduces significant security risks for which adequate solutions are yet to be found. New IIoT design methodologies also need to be developed, as sensor devices based on IPv6 protocols can be connected to any manufacturing process, without the need to use special gateway protocols. Traffic flows in industrial control systems and motion detection systems are deterministic, because their communication structure is known a priori. Routing and communication schedules are calculated in advance, to avoid packet collisions and to achieve global optimization of multiple traffic flows. This model differs from the classic IP Quality of Service (QoS) model which relies on selective buffering and packet rejection to allow end-to-end flow control. In order to provide the solution for these issues, Deterministic Networking (DetNet) [28] has been introduced as one of key concepts for future IIoT networks. Mechanisms applied in a particular DetNet scenario should limit packet transmission delays, while ensuring very high transmission reliability, which is of significant importance for Machine-to-Machine (M2M) operations. Moreover, novel solutions that provide ML-based crosslayer optimization in IIoT networks will enhance overall performances and increase efficiency [29].

Scheduled transmission in IIoT networks plays an important role towards establishing deterministic operations. New MAC modes are expected to provide high reliability with dedicated communication paths, data transmissions deterministic latency, and multichannel access. In particular, the TSCH mode on the MAC sublayer is created to support applications such as industrial automation and process control [30, 31]. The TSCH uses the combination of time synchronization and channel hopping to support deterministic delay guarantees, communication reliability and high network throughput. Channel hopping combats external interference and multipath fading and improves the communication reliability. The TSCH enables an ultra-low duty cycle less than 0.1%, thus extending battery life by up to 10 years. Most of the existing 6TiSCH implementations use the 2.4 GHz band, with 16 frequencies available. This multichannel transmission approach increases network capacity as it allows multiple communications at different channel offsets. The communication in a 6TiSCH network is orchestrated by a schedule. A slot frame consists of a matrix of cells of equal length (typically 10 ms), each cell being defined by a pair of timeslot and channel offsets. Slot frames repeat over time to enable nodes to have periodic access to the medium. TSCH defines two types of cells: dedicated and shared. A dedicated cell is contention-free provided that only one transmitter can send a packet. If cells are shared between multiple nodes, then the random access mechanism is applied. Different strategies have been proposed by the research community to provide advanced scheduling and routing mechanisms [32, 33, 34, 35] since the standard does not propose any optimized configuration for certain application domains.

In a 6TiSCH network, the creation of routing structure is

based on the IPv6 Routing Protocol for Low-power and lossy networks (RPL) protocol [36]. The long-term network stability strongly depends on the synergy between TSCH and RPL procedures. Here we would also like to emphasize the impact of selecting the right metric in order to estimate the link quality, and particularly to provide a stable routing topology. In our experimental activities, special attention has been given to this task. The overall network formation process highly influences the energy efficiency of 6TiSCH networks.

3.1 IEEE 802.15.4g

The IEEE 802.15.4-2015 standard revision, the IEEE 802.15.4g [20], defines a new set of three PHYs targeting outdoor low data rate wireless Smart Utility Network (SUN) applications. SUNs provide support for multiple applications to operate over shared network resources, while enabling two-way outdoor communications among measurement and control devices. The IEEE 802.15.4g standard introduces three PHYs: Multi-rate Multi-regional Offset Quadrature Phase Shift Keying (MR-OQPSK), Multi-rate Multi-regional Frequency Shift Keying (MR-FSK) and Multi-rate Multi-regional Orthogonal Frequency Division Multiplexing (MR-OFDM); where MR stands for communication in multiple bands and on multiple data rates. Its aim is to provide interoperability among differently capable networks by changing modulation and/or data rate on a packet-by-packet basis [20]. FSK and O-QPSK PHYs provide compatibility with legacy systems since these PHYs have already been widely used in low-power devices. On the other side, OFDM PHY has been traditionally used in complex wireless systems, but now is entering into the field of low-power wireless networks [37].

IEEE 802.15.4.g provides communication in license-free 700-1000 MHz and 2.4 GHz frequency bands and use of multiple data rates from 40 kb/s to 800 kb/s. It specifies the maximum length of a payload of 2047 bytes (B) so that a complete IPv6 packet can be transmitted without fragmentation, and coexistence with other systems operating in the same band (IEEE 802.11, 802.15 and 802.16).

3.1.1 FSK

FSK is a mandatory PHY implying that each IEEE 802.15.4g-device supports 2-FSK & 50 kb/s PHY configuration based on Gaussian FSK (GFSK) modulation with two or four levels thus providing constant amplitude of modulated signals [20]. This standard has introduced the novel Mode Switch (MS) mechanism that enables devices to change data rate and/or PHY on a packet-by-packet basis using FSK PHY. Based on this mechanism, PHY can be changed only for one packet and transceivers have to sup- port a specified PHY configuration. Two Physical Proto- col Data Unit (PPDU) formats are available depending on whether the MS mechanism is enabled (Fig. 1) or not (Fig. 2) [20].

A novel generic FSK mechanism provides support for the existing commercial PHY solutions and adoption of new PHY solutions as a consequence of technological progress or a regulatory change [25]. FSK PHY is commonly used for low data rates and high energy efficient applications, such as smart metering applications due to the constant envelope of the signal, and low implementation complexity [37]. Moreover, it is most common in the US in the 902-928 MHz band together with the Frequency Hopping Spread Spectrum (FHSS) technique [38].

		Octets
		2
Preamble	SFD	Defined by standard
SHR		PHR

Fig. 1 – Physical Protocol Data Unit (PPDU) format for FSK PHY with enabled mode switch mechanism.

		Octets	
		2	variable
Preamble	SFD	Defined by standard	PSDU
SHR		PHR	PHY payload

SFD - Start-of-Frame Delimiter
PSDU - PHY Service Data Unit
SHR - Synchronization Header
PHR - PHY Header

Fig. 2 – Physical Protocol Data Unit (PPDU) format for FSK PHY without enabled mode switch mechanism.

3.1.2 O-QPSK

The O-QPSK modulation technique shares the characteristics of IEEE 802.15.4 modulation being the most present in commercial devices [25]. The O-QPSK PHY provides multiple data rates using the Forward Error Correction (FEC), interleaving and Frequency Spread Spectrum Technique (FSST) [20]. Interleaving and FEC together increase robustness against burst errors and interrupt the correlation of consecutive bits [39]. This modulation type uses one of two FSSTs depending on the operating frequency band: Direct Sequence Spread Spectrum (DSSS) and Multiplexed Direct Sequence Spread Spectrum (MDSSS) [20]. Data transmission among legacy devices is ensured in the following frequency bands: 780, 915, 917, and 2450 MHz. Specified data and chip rates are presented in Table 2 [20].

Table 2 – O-QPSK data rates.

Chip rate [kchip/s]	Rate Mode	PSDU data rate [kb/s]
100	0/1/2/3	6.25/12.5/25/50
200	0/1/2/3	12.5/25/50/100
1000	0/1/2/3	31.25/125/250/500
2000	0/1/2/3/4	31.25/125/250/500/1000

3.1.3 OFDM

OFDM provides high data rates, spectrum efficiency and robustness against multipath fading and external interference in environments with frequency selective fading [40]. FSK and O-QPSK PHY are commonly used in low-power LR-WPANs due to their simplicity, low cost and good performances, whereas OFDM PHY is presented in systems with strong requirements for signal processing, memory and energy consumption (such as xDSL, LTE, WiMAX, PLC, and Wi-Fi) [18]. Therefore, OFDM has been applied in security and monitoring systems. OFDM consists of parallel data transmission with orthogonal subcarriers, each transporting one part of the information in a narrowband channel supporting robustness against multipath propagation, external interference and improves spectrum efficacy [37]. Advantages that OFDM provides are: higher data rates (50-800 kb/s), and the maximum PHY Service Data Unit (PSDU) length of 2047 B with no packet fragmentation [18].
An OFDM symbol (120 μs) consists of a base symbol (96 μs) and a Cyclic Prefix (CP). CP presents replication of the last 24 μs of the base symbol and is positioned in front of the base symbol. A cyclical feature and the long duration of an OFDM symbol make the OFDM PHY more robust against multipath propagation. This PHY provides four operating options (numbered from 1 to 4) with a set of Modulation Coding Schemes (MCSs) (numbered from 0 to 6). The MCS value specifies: the subcarrier modulation scheme (BPSK, QPSK, 16-QAM), the FEC coding rate (1/2 or 3/4) (mandatory), data rate and whether frequency repetition is applied [20]. Frequency repetition reduces the effective data rate, however, it improves robustness against multipath fading. Additionally, the OFDM PHY provides extended data rates for options 1 and 2 (1200, 1600 and 2400 kb/s) [20].

4. EXPERIMENT OVERVIEW

4.1 Experimental setup

This work is the extension of our previous research activities presented in [40], where the experiments were conducted to evaluate the preliminary results on the performance of multiple PHYs in the indoor environment. The experimental testbed comprises of open-source hardware and software platforms. Utilization of this approach has gained a lot of interest as it provides researchers with a significant tool for exploring and characterizing novel radio technologies [40]. The OpenMote-B device [41] (Fig. 3) consists of a Texas Instruments CC2538 System on Chip (SoC) and an Atmel AT86RF215 dual-band radio transceiver. The AT86RF215 provides transmission in both 2.4 GHz and sub-GHz frequency bands. The CC2538 SoC is based on an ARM Cortex-M3 micro-controller (32 MHz, 32 kB RAM, 512 kB Flash) and an IEEE 802.15.4-compatible radio transceiver; while AT86RF215 supports all IEEE 802.15.4g standardized PHYs [39, 42]. The OpenWSN [43] has been used as an open-source software tool. The branch [44] has developed support for certain IEEE 802.15.4g PHYs which has enabled us to run experiments.

For the performance evaluation, we have used the OpenTestBed scenario similar to [23, 45]. The OpenTestBed consists of five sets, where each set comprises of one Raspberry Pi 3 (RPi3) single-board computer and four attached OpenMote-B devices (nodes) (as shown in Fig. 3). One of the important functionalities of this OpenTestBed is to enable the remote control of nodes. RPi3 computers are connected to a Message Queuing Telemetry Transport (MQTT) server over a local Wi-Fi network. 20 OpenMote-B devices are deployed over two floors at the premises of the Faculty of Electrical Engineering in Banja Luka and their deployment position is shown in Fig. 4.

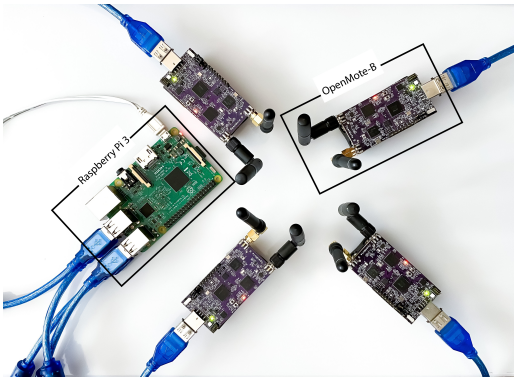

Fig. 3 – One OpenTestBed set.

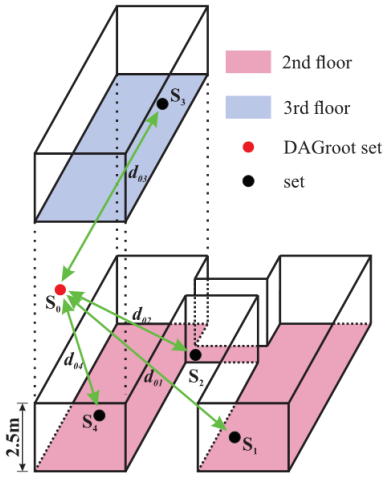

Fig. 4 – Experimental TestBed: Positions of sets across two floors at the premises of Faculty of Electrical Engineering.

One node is acting as a coordinator or Directed Acyclic Graph (DAG) root. One instance of the formed routing network is shown on Fig. 5, where the node depicted as D360 acts as a DAG root. Distances from the DAG root to each particular set S_i are highlighted in Fig. 4, where $d_{01} = 7.3$ m, $d_{02} = 9.5$ m, $d_{03} = 11.5$ m, and $d_{04} = 12.5$ m.

Several WiFi Access Points (APs) are deployed in the building. The nodes in such an indoor environment are the object of external interference due to Wi-Fi or other IEEE8021.5.4-PHY compliant networks. Therefore, we

have tested the network performance under different scenarios: during working hours and in the afternoon hours to avoid uncontrollable channel fluctuations. This deploying scenario mimics the possible distribution of sensors in a real industrial environment.

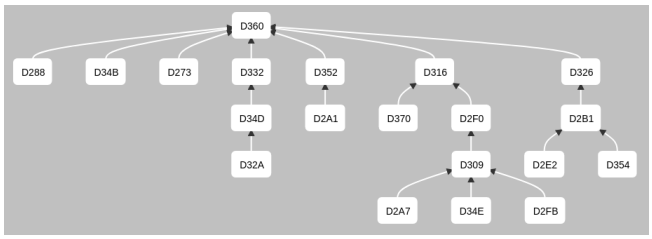

Fig. 5 – An example of the established routing network for the OFDM1-3 PHY scenario.

The following PHY configurations were tested:

- O-QPSK in 2.4GHz;
- FSK option 1 in sub-GHz;
- OFDM option 1 MCS 0 in sub-GHz;
- OFDM option 1 MCS 1 in sub-GHz;
- OFDM option 1 MCS 2 in sub-GHz;
- OFDM option 1 MCS 3 in sub-GHz.

4.2 Methodology

This extended experimental campaign aims at testing and verifying the OpenWSN implementation of supported PHYs. Table 3 lists the main characteristics of the tested PHYs; chip specifications define Tx power (P_{Tx}) and receiver sensitivity. P_{Tx} has been selected according to the results of initial test measurements. Tables 4 and 5 provide the PHY configuration parameters for all three tested modulation types.

Table 3 – The main parameters of tested PHYs.

PHY	Radio chip	P_{Tx} [dBm]	Data rate [kb/s]
O-QPSK 2.4GHz	CC2538	7	250
FSK 868MHz	AT86RF215	14.5	50
OFDM1 868MHz	AT86RF215	10	100/200/400/800

The following OpenWSN protocol stack parameters are specified for the experimental setup: slot-frame length (41), time slot duration (40 ms), packet queue size (15), and time period between two consecutive packets (5 s). Proper parameter settings highly influence system performance. The initial measurements were taken in order to select the adequate positions of nodes and to diminish the interference with other systems. The obtained results are based on the set of measurements during the steady-state of network. The node in the OpenTestBed set highlighted with a red circle in Fig. 4 was configured as DAG root and measurements lasted for 30 minutes. The *uinject* application collected data from each node in the network (except from DAG root) to measure network performance.

Table 4 – PHY parameters for FSK and O-QPSK.

PHY	FSK	O-QPSK
Data rate (kb/s)	50	250
Modulation index	1	N/A
Chip rate (kchips/s)	N/A	1000
Channel spacing (kHz)	200	2000
Note	Used FEC	Coding rate 1/2

Table 5 – PHY parameters for OFDM option 1.

Parameter	OFDM option 1
Bandwidth (kHz)	1094
Channel spacing (kHz)	1200
DFT size	128
Total/Pilot/Data pilots	104/96/8
MCS0 (kb/s) (BPSK, coding rate 1/2 with 4x frequency repetition)	100
MCS1 (kb/s) (BPSK, coding rate 1/2 with 2x frequency repetition)	200
MCS2 (kb/s) (QPSK, coding rate 1/2 with 2x frequency repetition)	400
MCS3 (kb/s) (QPSK, coding rate 1/2)	800

5. PERFORMANCE EVALUATION

This section summarizes the experimental performance evaluation focusing on the following metrics: network formation time, PDR, latency, and duty cycle. Moreover, we provide the relevant statistics for the latency and duty cycle. In order to compare the performance of the 6TiSCH stack on top of each selected PHY, we have used the corresponding OpenTestBed setup.

The network formation process consists of three phases: node synchronization, security handshake process, and rank acquisition. The DAG root broadcasts Enhanced Beacon (EB) messages and controls packets to advertise the presence of the network. These messages contain basic information (number of time slots in a slot frame, time slot duration, channel hopping sequence etc.) that allows new nodes to join the network and start the topology construction. The node is switching from one channel to another until it receives valid EB frame and becomes a TSCH synchronized node. Then, the security handshake process initiates the encryption mechanism. A rank acquisition process presents a time for which a node acquires routing information. The rank represents the relative distance between each node and the root node, and rank calculation depends on the Objective Function (OF).

In essence, the network formation process is the time required for the network to become fully functional [46]. To initiate this process, we turn on all the nodes and the gateway and flash them all at the same time. This procedure increases the network formation time since all nodes are trying to join at the same time causing a significant contention. On the other side, it allows us to observe the behavior of a network that is overloaded. Such a network mimics a possible scenario with a large number of nodes in a real industrial environment. The network formation time presents the time elapsed from the moment when the DAG root is selected to the moment when the DAG root has received a data packet from all nodes.

The results reflecting the network formation times are depicted in Fig. 6, where FSK 868 MHz, O-QPSK 2.4 GHz, OFDM1-0 868 MHz, OFDM1-1 868 MHz, OFDM1-2 868 MHz, and OFDM1-3 868 MHz PHY networks are fully formed in 6, 9, 7, 9, 14, and 10 minutes, respectively. Since FSK 868 MHz PHY provides a longer range than O-QPSK 2.4 GHz PHY, it discovers more nodes and synchronizes faster. The OFDM1-0 PHY network provides the best result among OFDM PHY configurations; this can be attributed to the utilization of the 4x frequency repetition technique. We have taken multiple measurements to obtain steady network conditions, which largely depend on the correct configuration of all the necessary parameters. The highest number of trials was in the case of the networks that tend to form slower, while the lowest number of repetitions was needed for the network that provides the fastest formation (FSK PHY network).

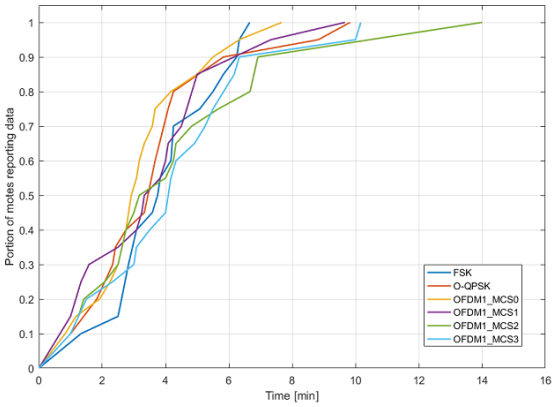

Fig. 6 – The network formation time for the tested PHYs: 6 min for FSK, 9 min for O-QPSK, 7 min for OFDM1-MCS0, 9 min for OFDM1-MCS1, 14 min for OFDM1-MCS2, and 10 min for OFDM1-MCS3.

The PDR is defined as the ratio between the number of successfully delivered data packets and the total number of transmitted data packets at the application layer. Table 6 presents PDR statistics averaged over all nodes for each PHY network. Considering the operating frequency band of O-QPSK 2.4 GHz PHY, the impact of external interference due to Wi-Fi or other technologies working in the same band is inevitable, which results in a few packet losses. In the case of OFDM1-2 PHY, instability of the network was a key problem as the routing network changed numerous times during the measurement process which resulted in a slightly lower PDR value (compared to other OFDM modes).

Table 6 – End-to-end Packet Delivery Ratio (PDR) [%] averaged over all nodes in the network.

PHY	PDR [%]
O-QPSK	99.17
FSK	100
OFDM1-0	100
OFDM1-1	100
OFDM1-2	99.69
OFDM1-3	100

The latency presents the time elapsed from the moment when the UDP packet is generated to the moment when it arrives at the DAG root node. The number of hops between the node and the root, and the number of retransmissions at each hop are the main factors affecting the latency. Fig. 7 shows a time-domain plot of the latency for the tested PHY networks. The results indicate that O-QPSK 2.4 GHz and OFDM1-2 868 MHz PHYs provide the highest latency, which directly corresponds to the lower values of PDR. Since the range is longer for FSK 868 MHz PHY and the impact of the interference is limited, the latency is lower. A decreased number of retransmissions and hops lead to the lower latency as well. In the case of OFDM PHY, the lower values of the MCS parameter provide the low latency which makes OFDM1-0 PHY the best among all OFDM options. Fig. 8 depicts the time-domain plot of the latency for O-QPSK 2.4GHz, FSK 868 MHz, and OFDM1-0 868 MHz PHYs only. Table 7 lists statistical properties of the latency for six tested PHY configurations. Fig. 9 depicts the cumulative distribution function of the latency for the tested PHY networks during the measurement period (30 minutes).

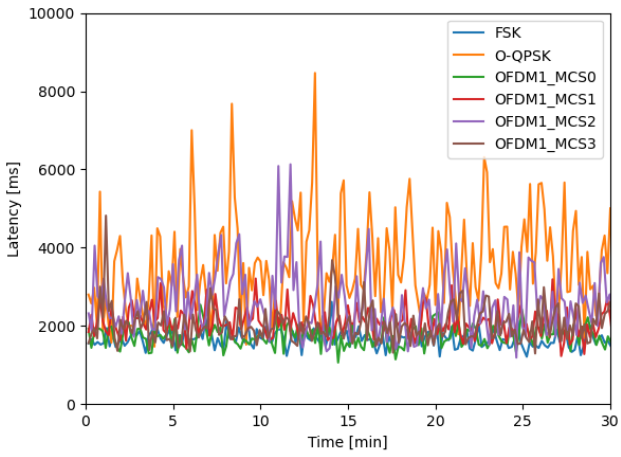

Fig. 7 – The latency for the tested PHY networks.

The duty cycle is the ratio of time the radio spends transmitting and the total duration for which the radio is on. The battery lifetime can be estimated by measuring the radio duty cycle. Although it cannot be a precise predic-

Table 7 – The latency [s] statistics over all nodes in the network, computed over the entire experiment.

	MIN	MAX	MEAN	MEDIAN	STD DEV	VARIANCE	STD ERROR
FSK	0.04	11.08	1.6678	1.48	1.0911	1.1906	0.0189
O-QPSK	0.08	24.92	2.8225	1.84	3.3849	11.4573	0.0584
OFDM1 MCS0	0.04	11.16	1.7383	1.48	1.2053	1.4527	0.0204
OFDM1 MCS1	0.04	15.28	2.0852	1.8	1.4871	2.2115	0.025
OFDM1 MCS2	0.08	24.6	2.1793	1.52	2.4262	5.8866	0.0426
OFDM1 MCS3	0.08	21.68	1.9879	1.56	1.7436	3.0401	0.0297

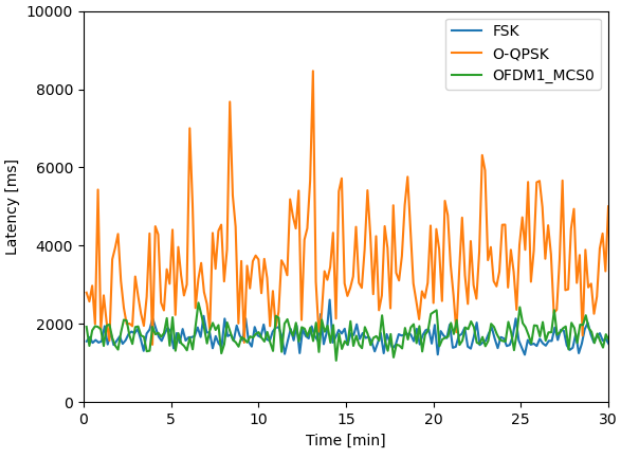

Fig. 8 – The latency for O-QPSK 2.4 GHz, FSK 868 MHz and OFDM1-0 868 MHz PHYs.

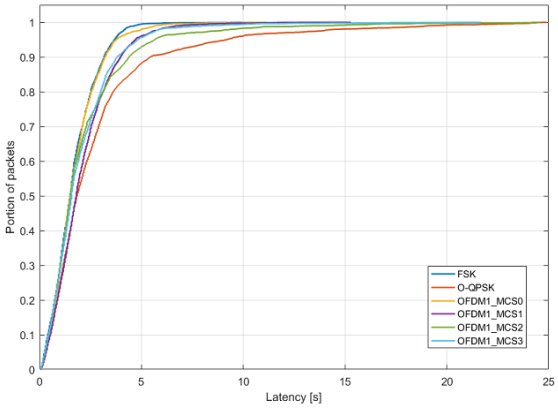

Fig. 9 – The cumulative distribution function of the latency.

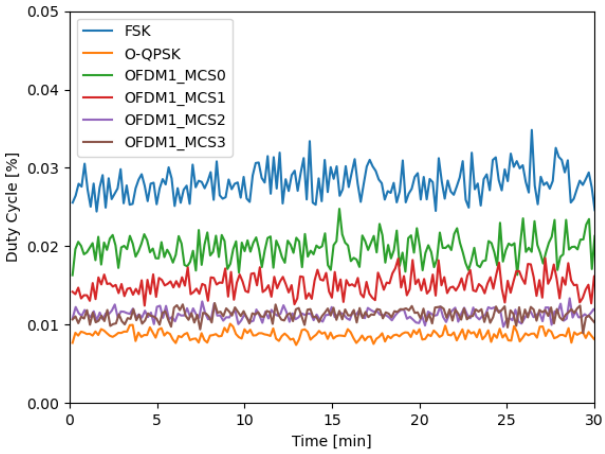

Fig. 10 – The duty cycle for the tested PHY networks.

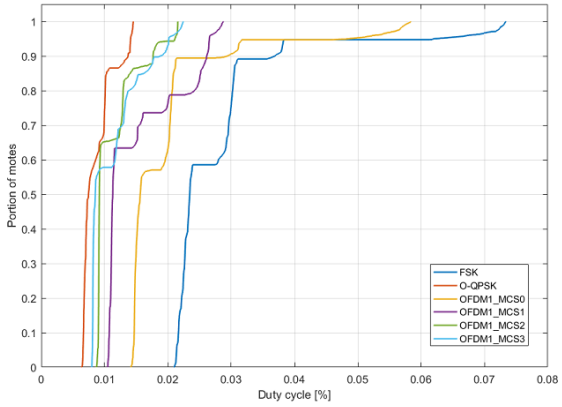

Fig. 11 – The cumulative distribution function of the duty cycle.

tor of a battery lifetime, the duty cycle is a good indicator of the energy efficiency of different PHYs. The measured radio duty cycle for all tested PHYs is depicted in Fig. 10. FSK 868 MHz and OFDM 868 MHz PHY networks have higher duty cycle values, therefore the battery lifetime is shorter in these cases. For different values of the MCS parameter, the OFDM 868 MHz PHY network examines different values of the duty cycle. The higher value of the MCS parameter provides higher data rates (Table 5) which results in the lower duty cycle, i.e., the higher energy efficiency. As Fig. 10 shows, O-QPSK 2.4 GHz PHY shows the best results in terms of energy efficiency. Table 8 lists statistical properties of the duty cycle for six tested PHY configurations. Fig. 11 shows the cumulative distribution function of the duty cycle for the tested PHY networks.

During the extensive experimental campaign, the network experienced problems such as incomplete network formation, drop out of nodes, and formation of isolated networks, eventually causing the network instability - thus requiring experiment repetition and accordingly parameter adjustment. The reason behind this is the nature of the TSCH protocol and the use of channel hopping which may increase the joining time of the nodes. These problems are mainly encountered in case of the

Table 8 – The duty cycle [%] statistics over all nodes in the network, computed over the entire experiment.

	MIN	MAX	MEAN	MEDIAN	STD DEV	VARIANCE	STD ERROR
FSK	0.021	0.0734	0.0281	0.0234	0.0109	1.1818e-04	1.8819e-04
O-QPSK	0.0064	0.0145	0.0087	0.0075	0.0024	5.8128e-06	4.0677e-05
OFDM1 MCS0	0.0142	0.0584	0.0197	0.0156	0.0092	8.5160e-05	1.5610e-04
OFDM1 MCS1	0.0105	0.0288	0.0151	0.0113	0.0061	3.7330e-05	1.0262e-04
OFDM1 MCS2	0.0087	0.0216	0.0113	0.0092	0.0036	1.2762e-05	6.1934e-05
OFDM1 MCS3	0.008	0.0224	0.0112	0.0085	0.0041	1.7205e-05	7.0455e-05

measurements during working hours with a high congestion of communication links and the movement of people causing interference and blockage, and thus the impact of noise and interference was significantly higher. During the life cycle of the 6TiSCH network, the nodes may be frequently de-synchronized for the above-mentioned reasons. Fig. 12 depicts one example of the routing network with dropped nodes and isolated networks.

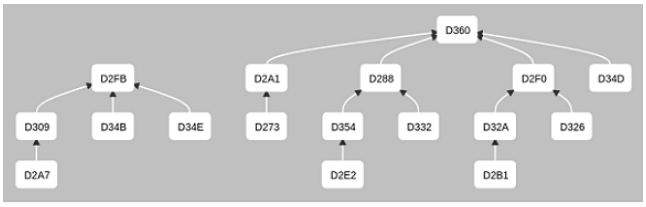

Fig. 12 – An example of the routing network failure for the FSK PHY scenario.

Such a significant impact of noise and interference during working hours results in poor performance for each PHY network in terms of latency and PDR. Figures 13 and 14 show a time-domain plot of the latency for the FSK 868 MHz and O-QPSK 2.4 GHz PHY networks, respectively, under different scenarios: during and after working hours. The higher presence of noise and interference during working hours caused higher latency values (Fig. 13 and Fig. 14). Table 9 lists statistical properties of the latency for the FSK 868 MHz and the O-QPSK 2.4 GHz PHY networks under different scenarios together with the corresponding PDR values. Table 10 lists the statistical properties of the duty cycle for the FSK 868 MHz and the O-QPSK 2.4 GHz PHY networks under different scenarios. The obtained results indicate that environmental conditions do not have a significant impact on the duty cycle metric. These observations should be taken into consideration for proper experiment configuration and performance evaluation.

The acquired dataset presented in this article and developed Python scripts for data analysis can be found at a public GitHub repository[1]. Data is formatted in Excel tables, pkl and text files for each tested PHY.

[1]https://github.com/MilicaL/OpenTestBed-6TiSCH

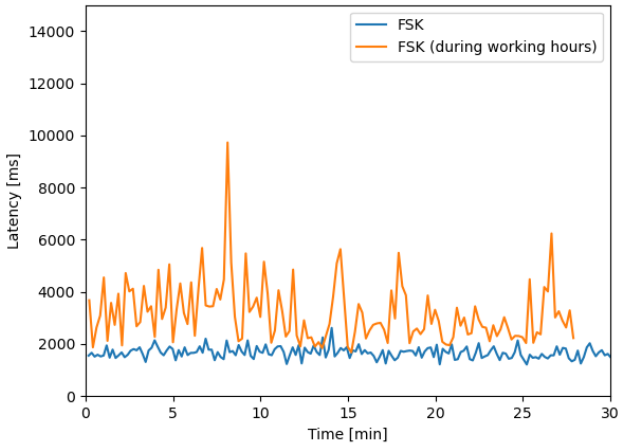

Fig. 13 – The latency of the FSK network under two different scenarios: during and after working hours.

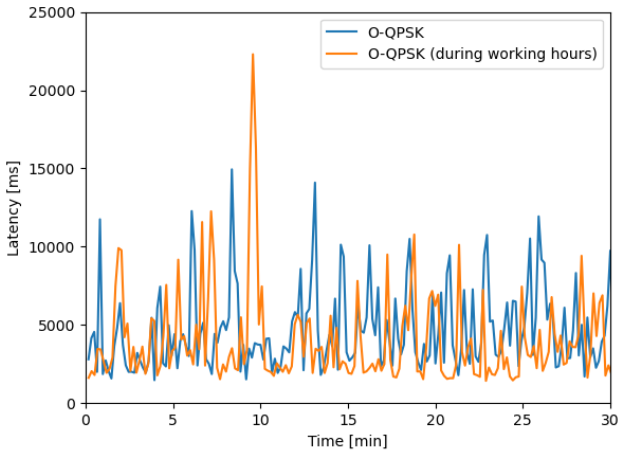

Fig. 14 – The latency of the O-QPSK network under two different scenarios: during and after working hours.

6. DISCUSSION

Performed multiple experiments have revealed the following observations: The FSK 868 MHz PHY exhibits the shortest network formation time; PDR statistics indicate that obtained values are very high for all PHYs, thus confirming the high reliability of 6TiSCH networks; the shortest latency is obtained for FSK 868 MHz and OFDM1-0 868

Table 9 – The latency [s] statistics and PDR values for the FSK and O-QPSK PHY networks under two different scenarios.

	MIN	MAX	MEAN	MEDIAN	STD.DEV	VARIANCE	STD.ERROR	PDR[%]
FSK	0.04	11.08	1.6678	1.48	1.0911	1.1906	0.0189	100
FSK (during working hours)	0.04	49.68	3.2203	2.2	4.4705	19.9856	0.0883	98.62
O-QPSK	0.08	24.92	2.8225	1.84	3.3849	11.4573	0.0584	99.17
O-QPSK (during working hours)	0.08	59.6	3.1123	1.84	5.8843	34.6246	0.1017	95.86

Table 10 – The duty cycle [%] statistics for the FSK and O-QPSK PHY networks under two different scenarios.

	MIN	MAX	MEAN	MEDIAN	STD.DEV	VARIANCE	STD.ERROR
FSK	0.021	0.0734	0.0281	0.0234	0.0109	1.1818e-04	1.8819e-04
FSK (during working hours)	0.0206	0459	0.0274	0.0232	0.0075	5.6418e-05	1.4768e-04
O-QPSK	0.0064	0.0145	0.0087	0.0075	0.0024	5.8128e-06	4.0677e-05
O-QPSK (during working hours)	0.0066	0.0181	0.0095	0.0071	0.0036	1.3184e-05	6.2198e-05

MHz PHYs; and the best duty cycle is attributed to O-QPSK 2.4 GHz PHY. The OFDM1-0 868 MHz PHY provides balanced results between FSK 868 MHz and O-QPSK 2.4 GHz PHYs. Since there is no single PHY layer that exhibits the best performance for all measured metrics, the possible approach could be to change the PHY and/or data rate on a packet-by-packet basis.

The collected data provide us with the opportunity to analyze the results for the applications in the indoor environment. Here, the focus is on the indoor application with high density traffic in the 2.4 GHz frequency band. We can define which PHY and its configuration is the most appropriate for our set-up environment and application requirements. The obtained data is a showcase for the node deployment similar to Fig. 4, so these results cannot be generalized. The aim of this paper is also to indicate that no single PHY can achieve optimal performance for all relevant network metrics thus opening the door to investigate diverse multi-PHY network scenarios.

During this experimentation campaign, we have noticed the node's tendency to frequently change the parent node thus introducing the network instability. Moreover, nodes have needed to re-synchronize continuously. Therefore, this issue calls for the implementation of novel parent selection mechanisms and different slot sizes as proposed in [47]. The observed network behavior during this measurement campaign indicates the importance of proper node positioning and careful selection of network parameters. The full compliance of open-source implementations with the 6TiSCH standards is another challenging issue.

7. CONCLUSION

Diverse IoT applications (such as smart cities, automation of industrial processes, agriculture, healthcare, etc.) have different requirements in terms of data rate, throughput, reliability, coverage, etc. Recently, the TSCH standardization activities have started to consider the support for multiple physical layers. This paper aims at providing results obtained in an extensive experimental campaign by testing the performance of a multi-PHY 6TiSCH network. For experimentation purposes, OpenWSN and OpenMote-B platforms are deployed in the indoor environment. The obtained results are encouraging, particularly in terms of high PDR for all tested PHYs thus introducing the possibility to select the PHY that suits best for particular IIoT applications. Advanced and novel techniques will enable the selection of a proper PHY to ensure balanced performance and to accommodate diverse network requirements. As a part of future work, we plan to investigate the use of ML for joint scheduling and routing algorithms.

ACKNOWLEDGEMENT

This work has been performed under the framework of COST Action CA20120—Intelligence-Enabling Radio Communications for Seamless Inclusive Interactions (INTERACT).

REFERENCES

[1] C. Lin et al. "Key design of driving industry 4.0: joint energy-efficient deployment and scheduling in group-based industrial wireless sensor networks". In: *IEEE Communications Magazine* 54.10 (2016), pp. 46–52.

[2] Hui Zhou et al. "Machine Learning for Massive Industrial Internet of Things". In: *IEEE Wireless Communications* 28.4 (2021), pp. 81–87. DOI: 10.1109/MWC.301.2000478.

[3] Basheer Qolomany et al. "Trust-Based Cloud Machine Learning Model Selection for Industrial IoT and Smart City Services". In: *IEEE Internet of Things Journal* 8.4 (2021), pp. 2943–2958. DOI: 10.1109/JIOT.2020.3022323.

[4] Xiaokang Wang et al. "ADTT: A Highly Efficient Distributed Tensor-Train Decomposition Method for IIoT Big Data". In: *IEEE Transactions on Industrial Informatics* 17.3 (2021), pp. 1573–1582. DOI: 10.1109/TII.2020.2967768.

[5] Tian Wang et al. "Big Data Cleaning Based on Mobile Edge Computing in Industrial Sensor-Cloud". In: *IEEE Transactions on Industrial Informatics* 16.2 (2020), pp. 1321–1329. DOI: 10.1109/TII.2019.2938861.

[6] Yyi Kai Teoh, Sukhpal Singh Gill, and Ajith Kumar Parlikad. "IoT and Fog Computing based Predictive Maintenance Model for Effective Asset Management in Industry 4.0 using Machine Learning". In: *IEEE Internet of Things Journal* (2021), pp. 1–1. DOI: 10.1109/JIOT.2021.3050441.

[7] Alexander Willner and Varun Gowtham. "Toward a Reference Architecture Model for Industrial Edge Computing". In: *IEEE Communications Standards Magazine* 4.4 (2020), pp. 42–48. DOI: 10.1109/MCOMSTD.001.2000007.

[8] Gregory Falco, Carlos Caldera, and Howard Shrobe. "IIoT Cybersecurity Risk Modeling for SCADA Systems". In: *IEEE Internet of Things Journal* 5.6 (2018), pp. 4486–4495. DOI: 10.1109/JIOT.2018.2822842.

[9] Shahid Latif et al. "A Novel Attack Detection Scheme for the Industrial Internet of Things Using a Lightweight Random Neural Network". In: *IEEE Access* 8 (2020), pp. 89337–89350. DOI: 10.1109/ACCESS.2020.2994079.

[10] Ke Huang et al. "Building Redactable Consortium Blockchain for Industrial Internet-of-Things". In: *IEEE Transactions on Industrial Informatics* 15.6 (2019), pp. 3670–3679. DOI: 10.1109/TII.2019.2901011.

[11] Bin Cao et al. "A Many-Objective Optimization Model of Industrial Internet of Things based on Private Blockchain". In: *IEEE Network* 34.5 (2020), pp. 78–83. DOI: 10.1109/MNET.011.1900536.

[12] Wenchao Xia et al. "Mobile Edge Cloud-Based Industrial Internet of Things: Improving Edge Intelligence with Hierarchical SDN Controllers". In: *IEEE Vehicular Technology Magazine* 15.1 (2020), pp. 36–45. DOI: 10.1109/MVT.2019.2952674.

[13] Juan Luis Herrera et al. "Optimizing the Response Time in SDN-Fog Environments for Time-Strict IoT Applications". In: *IEEE Internet of Things Journal* 8.23 (2021), pp. 17172–17185. DOI: 10.1109/JIOT.2021.3077992.

[14] *Minimal IPv6 over the TSCH Mode of IEEE 802.15.4e (6TiSCH) Configuration*. RFC 8180. May 2017. DOI: 10.17487/RFC8180.

[15] "IEEE Standard for Local and metropolitan area networks–Part 15.4: Low-Rate Wireless Personal Area Networks (LR-WPANs) Amendment 1: MAC sublayer". In: *IEEE Std 802.15.4e-2012 (Amendment to IEEE Std 802.15.4-2011)* (2012), pp. 1–225. DOI: 10.1109/IEEESTD.2012.6185525.

[16] Pascal Thubert. *An Architecture for IPv6 over the Time-Slotted Channel Hopping Mode of IEEE 802.15.4 (6TiSCH)*. RFC 9030. May 2021. DOI: 10.17487/RFC9030. URL: https://www.rfc-editor.org/info/rfc9030.

[17] "IEEE Standard for Low-Rate Wireless Networks". In: *IEEE Std 802.15.4-2015 (Revision of IEEE Std 802.15.4-2011)* (2016), pp. 1–709. DOI: 10.1109/IEEESTD.2016.7460875.

[18] Pere Tuset-Peiró et al. "Experimental Interference Robustness Evaluation of IEEE 802.15.4-2015 OQPSK-DSSS and SUN-OFDM Physical Layers for Industrial Communications". In: *Electronics* 8.9 (2019). ISSN: 2079-9292. DOI: 10.3390/electronics8091045.

[19] Pere Tuset-Peiro et al. "Reliability Through Modulation Diversity: Can Combining Multiple IEEE 802.15.4-2015 SUN Modulations Improve PDR?" In: June 2020. DOI: 10.1109/ISCC50000.2020.9219719.

[20] "IEEE Standard for Local and metropolitan area networks–Part 15.4: Low-Rate Wireless Personal Area Networks (LR-WPANs) Amendment 3: Physical Layer (PHY) Specifications for Low-Data-Rate, Wireless, Smart Metering Utility Networks". In: *IEEE Std 802.15.4g-2012 (Amendment to IEEE Std 802.15.4-2011)* (2012), pp. 1–252.

[21] Ruan Delgado Gomes, Pere Tuset-Peiró, and Xavier Vilajosana. "Improving Link Reliability of IEEE 802.15.4g SUN with Adaptive Modulation Diversity". In: *2020 IEEE 31st Annual International Symposium on Personal, Indoor and Mobile Radio Communications*. 2020, pp. 1–7. DOI: 10.1109/PIMRC48278.2020.9217301.

[22] Domenico Solimini et al. "Towards Reliable IEEE 802.15.4g SUN with Re-transmission Shaping and Adaptive Modulation Selection". In: *Journal of Signal Processing Systems* (May 2021). DOI: 10.1007/s11265-021-01665-z.

[23] Mina Rady et al. "g6TiSCH: Generalized 6TiSCH for Agile Multi-PHY Wireless Networking". In: *IEEE Access* 9 (2021), pp. 84465–84479. DOI: 10.1109/ACCESS.2021.3085967.

[24] M. Rady et al. "No Free Lunch—Characterizing the Performance of 6TiSCH When Using Different Physical Layers". In: *Sensors* 20.17 (2020). ISSN: 1424-8220. DOI: 10.3390/s20174989.

[25] Milica Lekić and Gordana Gardašević. "Experimental Performance Evaluation of IEEE 802.15.4g Applications Using OpenMote-B Devices". In: *Proceedings of the Twenty-nine International Electrotechnical and Computer Science Conference ERK 2020, ISSN: 2591-0442 (online)*. Available: https://communications.etf.unibl.org/Milica_Lekic%20ERK2020%20FinalVersion.pdf. Sept. 2020.

[26] Francesca Righetti et al. "Performance Measurements of IEEE 802.15.4g Wireless Networks". In: *2019 IEEE 20th International Symposium on "A World of Wireless, Mobile and Multimedia Networks" (WoWMoM)*. 2019, pp. 1–6. DOI: 10.1109/WoWMoM.2019.8793051.

[27] Dries Van Leemput et al. "Adaptive multi-PHY IEEE802.15.4 TSCH in sub-GHz industrial wireless networks". In: *Ad Hoc Networks* 111 (2021), p. 102330. ISSN: 1570-8705. DOI: https://doi.org/10.1016/j.adhoc.2020.102330.

[28] N. Finn and P. Thubert. *Deterministic Networking Problem Statement*. Internet-Draft. Work in Progress. Internet Engineering Task Force, Sept. 2017.

[29] Arslan Musaddiq et al. "Reinforcement Learning-Enabled Cross-Layer Optimization for Low-Power and Lossy Networks under Heterogeneous Traffic Patterns". In: *Sensors* 20.15 (2020). ISSN: 1424-8220. DOI: 10.3390/s20154158.

[30] Rodrigo Teles Hermeto, Antoine Gallais, and Fabrice Theoleyre. "Scheduling for IEEE802.15.4-TSCH and Slow Channel Hopping MAC in Low Power Industrial Wireless Networks: A Survey". In: *Comput. Commun.* 114.C (Dec. 2017), pp. 84–105. ISSN: 0140-3664. DOI: 10.1016/j.comcom.2017.10.004.

[31] Maria Rita Palattella et al. "On Optimal Scheduling in Duty-Cycled Industrial IoT Applications Using IEEE802.15.4e TSCH". In: *IEEE Sensors Journal* 13.10 (2013), pp. 3655–3666.

[32] Tijana Devaja et al. "Scheduling in 6TiSCH Networks via Max-Product Message-Passing". In: *IEEE EUROCON 2019 -18th International Conference on Smart Technologies*. 2019, pp. 1–6. DOI: 10.1109/EUROCON.2019.8861979.

[33] Gordana Gardašević et al. "Experimental Characterization of Joint Scheduling and Routing Algorithm Over 6TiSCH". In: *2018 European Conference on Networks and Communications (EuCNC)*. 2018, pp. 424–428. DOI: 10.1109/EuCNC.2018.8442481.

[34] Dragan Vasiljević and Gordana Gardašević. "Packet Aggregation-Based Scheduling in 6TiSCH Networks". In: *IEEE EUROCON 2019 -18th International Conference on Smart Technologies*. 2019, pp. 1–5. DOI: 10.1109/EUROCON.2019.8861910.

[35] Anderson Rocha Ramos, Fernando J. Velez, and Gordana Gardašević. "Source Routing Minimum Cost Forwarding Protocol over 6TiSCH Applied to the OpenMote-B Multi-hop Platform". In: *2019 IEEE 30th Annual International Symposium on Personal, Indoor and Mobile Radio Communications (PIMRC)*. 2019, pp. 1–6. DOI: 10.1109/PIMRC.2019.8904356.

[36] T. Winter et al. *RPL: IPv6 Routing Protocol for Low-Power and Lossy Networks*. RFC 1654. RFC Editor, Mar. 2012, pp. 1–56.

[37] J. Muñoz et al. "Overview of IEEE802.15.4g OFDM and its Applicability to Smart Building Applications". In: *2018 Wireless Days (WD)*. 2018, pp. 123–130.

[38] Kuor-Hsin Chang and Bob Mason. "The IEEE 802.15.4g Standard for Smart Metering Utility Networks". In: *2012 IEEE Third International Conference on Smart Grid Communications (SmartGridComm)*. 2012, pp. 476–480. DOI: 10.1109/SmartGridComm.2012.6486030.

[39] Pere Tuset-Peiró et al. "A Dataset to Evaluate IEEE 802.15.4g SUN for Dependable Low-Power Wireless Communications in Industrial Scenarios". In: *Data* 5.3 (July 2020), p. 64. ISSN: 2306-5729. DOI: 10.3390/data5030064.

[40] Milica Lekić and Gordana Gardašević. "Performance Evaluation of 6TiSCH Network with Multiple Physical Layers". In: *2021 International Balkan Conference on Communications and Networking (BalkanCom)*. 2021, pp. 138–142. DOI: 10.1109/BalkanCom53780.2021.9593227.

[41] Xavier Vilajosana et al. "OpenMote: Open-Source Prototyping Platform for the Industrial IoT". In: Sept. 2015. ISBN: 978-3-319-25066-3. DOI: 10.1007/978-3-319-25067-0_17.

[42] Pere Tuset-Peiró, Xavier Vilajosana, and Thomas Watteyne. "OpenMote+: A Range-Agile Multi-Radio Mote". In: *Proceedings of the 2016 International Conference on Embedded Wireless Systems and Networks*. EWSN '16. Graz, Austria: Junction Publishing, 2016, pp. 333–334. ISBN: 9780994988607.

[43] OpenWSN. *The official web page of the OpenWSN project*. www.openwsn.atlassian.net/wiki/spaces/OW/overview. (Visited on 01/25/2022).

[44] OpenWSN-fw. *GitHub repositorium of the OpenWSN branch*. github.com/minarady1/openwsn-fw/tree/develop_FW-866_v2/projects. (Visited on 01/05/2022).

[45] Mina Rady et al. "6DYN : 6TiSCH with Heterogeneous Slot Durations". In: *Sensors* 21.5 (2021). ISSN: 1424-8220. DOI: 10.3390/s21051611.

[46] Yasuyuki Tanaka et al. "Accelerating 6TiSCH Network Formation". In: *DCOSS 2021 : 17th Annual International Conference on Distributed Computing in Sensor Systems*. Virtual, France, July 2021, pp. 18–24. DOI: 10.1109/DCOSS52077.2021.00016. URL: https://hal.inria.fr/hal-03538225.

[47] Glenn Daneels et al. "Parent and PHY Selection in Slot Bonding IEEE 802.15.4e TSCH Networks". In: *Sensors* 21.15 (2021). ISSN: 1424-8220. DOI: 10.3390/s21155150.

AUTHORS

Milica Lekić (Student Member, IEEE) received B.Sc. and M.Sc. degrees in electrical engineering from the Faculty of Electrical Engineering, University of Banja Luka, in 2017 and 2020, respectively. She is currently pursuing a Ph.D. degree with the Department of Electronic Systems, Norwegian University of Science and Technology, Norway. Her research interests include the Internet of Things and molecular communications.

Gordana Gardašević (Member, IEEE) received a Ph.D. degree in electrical engineering from the Faculty of Electrical Engineering (FEE), Banja Luka, Bosnia and Herzegovina, in 2008. She was a doctoral research fellow at the School of Electrical and Computer Engineering, National Technical University of Athens (NTUA), Greece, from 2006 to 2008. During the academic year 2013-2014, she was a post-doctoral fellow at the University of Bologna. She is a full professor and Chief of Department of Telecommunications at FEE. Prof. Gardašević is the author of three books and two monographs. She has coordinated and participated in a number of international and national research teams and projects. Her research interests include Internet of Things (IoT) protocols and applications, Industrial IoT, IoT for healthcare, next generation network architectures and applications, cross-layer protocol design, wireless sensor networks. Prof. Gardašević is the author or co-author of more than 80 peer-reviewed journal and conference papers, and serves as a journal editorial board member and guest editor, reviewer for several international impact-factor journals and is a TCP member for various international conferences and workshops.

Milan Mlađen (Student Member, IEEE) received a B.Sc. degree in electrical engineering from the Faculty of Electrical Engineering (FEE), University of Banja Luka, Bosnia and Herzegovina, in 2020. He is currently pursuing an M.Sc. degree with the Department of Telecommunications at FEE and is currently working as a research and teaching assistant with the Department of Telecommunications at FEE. His research interests include the Internet of Things (IoT), Industrial IoT, and wireless sensor networks.